Bulletin of Earthquake Engineering (2023) 21:5545–5571
https://doi.org/10.1007/s10518-023-01740-9

ORIGINAL ARTICLE

Effectiveness of structural walls in improving the serviceability of a seismically-retrofitted RC building

Ahmet Şimşek[1] · Özgür Yurdakul[2] · Burak Duran[3] · Onur Tunaboyu[1] · Suat Yıldırım[4] · Özgür Avşar[1]

Received: 23 November 2022 / Accepted: 10 July 2023 / Published online: 24 July 2023

Abstract
A moderate earthquake with a magnitude M_w of 6.8 hit the Elazig Province of Turkey on January 24th, 2020, causing fatalities and structural damage/failure. Following the earthquake, a field reconnaissance was conducted at the Administration and Operation Campus of Karakaya Dam, which is 19 km from the earthquake epicenter. The exhibited performances in two side-by-side nominally identical reinforced concrete (RC) buildings with the same material properties and soil conditions differed significantly. The main reason lies in the preventive action taken before the earthquake in one of the buildings. The building retrofitted with additional structural walls had a slight/no damage level. However, the non-retrofitted building suffered severe damage due to large cracks in numerous infill walls, some of which were exposed to partial collapse. That makes the non-retrofitted building unserviceable, requiring evacuation after the earthquake. The field-observed building damage was compared with the seismic performances acquired from their refined numerical models for the recorded ground motions. The photographic documentation exposing the entire performance and damage level in non-retrofitted and retrofitted buildings was quantified by static pushover and nonlinear response history analyses. The post-earthquake performance of nonstructural members in retrofitted and non-retrofitted buildings was simulated with reasonable accuracy.

Keywords Retrofit · Structural wall · Seismic performance · Substandard · Numerical study

1 Introduction

Past destructive earthquakes have shown that a large portion of building stock in developed and developing countries is well below the desired target performance level specified by seismic codes and guidelines (Rossetto and Peiris 2009; Garcia et al. 2010; Shahzada et al. 2010; Naseer et al. 2010; Ozturk 2013; Yılmaz and Avşar 2013; Ricci et al. 2011; Avşar and Tunaboyu 2013; Yurdakul et al. 2021). Field investigations after moderate to severe earthquakes revealed the poor seismic performance of substandard buildings due to their old-fashioned design and construction principles, which do not comply even with the former design provisions. These buildings have critical structural deficiencies, such as

Extended author information available on the last page of the article

low-strength concrete, plain reinforcing bars usually with a significant level of corrosion, insufficient transverse reinforcement with improper detailing, and structural irregularities, among others. Consequently, such deficiencies make them vulnerable to seismic actions, jeopardizing the seismic performance of the buildings. As a result of the substandard building stock, even a moderate earthquake with a magnitude M_w of 6.8—which occurred in the Sivrice district of Elazığ Province in Eastern Turkey on January 24th, 2020—caused fatalities and property loss due to premature member failures in substandard buildings. This, in turn, triggered the overall structural failure. According to a preliminary survey in 2020 performed by the Ministry of Environment and Urbanisation (MoEU), the number of buildings with slight damage was reported to be 17,021, while 1,492 buildings had moderate damage, and 8,396 buildings had severe damage. Additionally, 821 buildings were marked for immediate demolition or collapse following the earthquake, as reported by the Anadolu Agency in 2020. Socio-economic aspects such as displacing from damaged buildings, finding safer and available shelter causing disruptions in public life, and increasing housing prices are typical results of having an excessive number of unserviceable buildings. Such adverse effects should be eliminated by replacing the substandard structures with code-compliant ones. However, demolition and re-construction of those structures are not always practical due to economic constraints, downtime, and applicability issues. In certain situations, immediate intervention is required for a building to be serviceable after an earthquake. For this purpose, retrofitting methodologies can be the solution to upgrade structural performance and lessen seismic risk (Duran et al. 2019). Depending on the required performance level, compatibility with the existing structural system, feasibility of the conditions, availability of materials and technology, and the level of seismic intervention can be selected at the local or global level (Thermou and Elnashai 2006). Local retrofit techniques can be implemented in a group of members to increase their capacity (Del Vecchio et al. 2014; Del Zoppo et al. 2017; Lee et al. 2017; Yurdakul et al. 2019, 2020; De Risi et al. 2020). Alternatively, global retrofit techniques are used to enhance the overall structural behavior with the addition of a bracing system (Maheri et al. 2003; Mazzolani et al. 2009; Durucan and Dicleli 2010; Akbari et al. 2015), structural walls (Avşar and Tunaboyu 2013; Sonuvar et al. 2004; Kara and Altin 2006; Altin et al. 2008; Kaltakci et al. 2008; Strepelias et al. 2014; Cerè et al. 2022) or other advanced systems (Cao et al. 2022; Joseph et al. 2022).

Previous studies demonstrated the effectiveness of structural walls (a commonly applied method) by comparing the response of RC buildings with and without structural walls through experimental methods, numerical approaches, and field observations. However, the uncertainties associated with measured, computed, and observed response quantities have prevented a full characterization of the effectiveness of added structural walls. Moreover, the differences in building material properties, soil conditions, and structural configurations may also significantly affect the seismic performance, making it challenging to attribute the improvement in the seismic performance solely to the added structural walls. Despite extensive research in this area, studies have lacked the field observation and assessment of the seismic performance of two side-by-side nominally identical buildings with the same material properties, structural geometry, and configurations. From the authors' best knowledge, no specific research has been conducted to investigate the effectiveness of adding structural walls by comparing the seismic response of two nominally identical buildings, one retrofitted with structural walls and the other one non-retrofitted, following an earthquake. This approach ensures that any observed difference in seismic performance can be attributed solely to the added structural walls, rather than to other variables such as building material properties, soil conditions, location, or structural configurations.

This study investigates the effectiveness of adding structural walls as a seismic retrofitting approach through field observations and numerical analysis of two nominally identical 4-story RC residential buildings with the same material properties, soil conditions, and location. One building was retrofitted by adding structural walls before the earthquake, while the other building remained unaltered. The novelty of this study lies in the comparison of the evaluated performances via numerical analysis of damage levels of both retrofitted and non-retrofitted buildings, considering all the relevant factors that may affect seismic performance. The result of this study provides a comprehensive understanding of the effectiveness of seismic retrofitting methods. The study's framework includes photographic documentation of the entire performance and damage levels of both buildings, static pushover and nonlinear response history analyses, and the verification of numerical models by comparing the observed damage and computed performances of both retrofitted and non-retrofitted buildings.

2 Motivation for research

The two side-by-side nominally identical, substandard RC residential buildings are located in the Karakaya Dam administration and operation campus, which is about 19 km from the epicenter of the Elazığ-Sivrice Earthquake in Turkey, which occurred on January 24th, 2020. These buildings are of interest both because they were closer to the earthquake epicenter, and due to their existing structural deficiencies. In addition, the post-earthquake conditions of these two nominally identical buildings deserve special attention from a structural engineering perspective. The non-retrofitted building suffered moderate damage with the partial collapse of infill walls and slight damage on the structural components, which makes this building unserviceable. On the other hand, the retrofitted building (strengthened by additional structural walls) was in a state of slight/no damage after the earthquake with no interruption in serviceability. The effectiveness of the global seismic retrofit technique by additional structural walls was clearly observed and documented through the on-site investigations. Moreover, the observed performances of these identical buildings are reproduced by computer simulations (e.g., pushover analyses and nonlinear response history analyses using the recorded ground motion data). The originality of the study lies in the comparisons of the observed and simulated seismic response of these two nominally identical RC buildings, one of which was retrofitted with structural walls before the earthquake, while the other was not, with no variability effects since both buildings have the same material properties, structural configuration, and geometry. This study also compared the serviceability limits of nonstructural elements in the seismic codes with reproduced deformations via an analytical model to unveil the effectiveness of additional structural walls as a global retrofit strategy. The simulated nonstructural deformations in the retrofitted building satisfy the serviceability limit state, while the quantified deformations exceed that limit in the non-retrofitted building. These findings are supported by photographic documentation of the buildings' actual performance following the earthquake.

3 Earthquake data and recorded ground motions

On January 24th, 2020, a moderate earthquake with a magnitude of M_w 6.8 occurred in the Sivrice District of Elazığ, located in the eastern region of Turkey. The earthquake struck at 08:55 PM (GMT + 3) local time. Sivrice district is the closest residential area

to the epicenter of the earthquake (38.3593 °N, 39.0630 °E), and the focal depth of the earthquake was 8.06 km (DEMP (2020)). This earthquake occurred on the Eastern Anatolian Fault Line, one of the most active faults in Turkey (Fig. 1). After the main shock of the Sivrice-Elazığ earthquake, 3,079 aftershocks having a magnitude M_w greater than 3 and 26 aftershocks having a magnitude M_w greater than 4 occurred within a month (Yurdakul et al. 2021). The death toll reached 41 just after the earthquake, while more than 1,607 people were injured (Anadolu Agency (2020)). Among the investigated 61,152 buildings, 10,709 were marked as moderately damaged, severely damaged, or collapsed (MoEU (2020)). As a socio-economic result, this moderate-intensity earthquake significantly disrupted and affected public life, resulting in both loss of life and property.

During the Sivrice-Elazığ Earthquake, a total of 235 strong-motion stations recorded the acceleration time series. From these, three stations were selected for nonlinear time history analyses based on their relatively high seismic intensities in terms of peak ground acceleration (PGA) and peak ground velocity (PGV). These stations are Elazığ-Center (Station ID: #2301), Elazığ-Sivrice (Station ID: #2308), and Malatya-Pütürge (Station ID: #4404). The acceleration-time series of these three ground motion records are presented in Fig. 2a–c. The geometric mean of the response spectra of the two horizontal components of these three records was compared with the design spectra for 475-year (DD2) and 72-year (DD3) return period earthquakes specified in the current version of the seismic design code (TBEC (2018) for the indicated soil conditions (Fig. 2a–c). The characteristics of ground motion recordings of the three stations are given in Tables 1 and 2. Upon comparing the geometric mean of the response spectra with the design spectra, it is apparent that the spectral acceleration values of the recorded data fall within the design spectra of 475-year (design earthquake) and 72-year (serviceability earthquake) return period earthquakes.

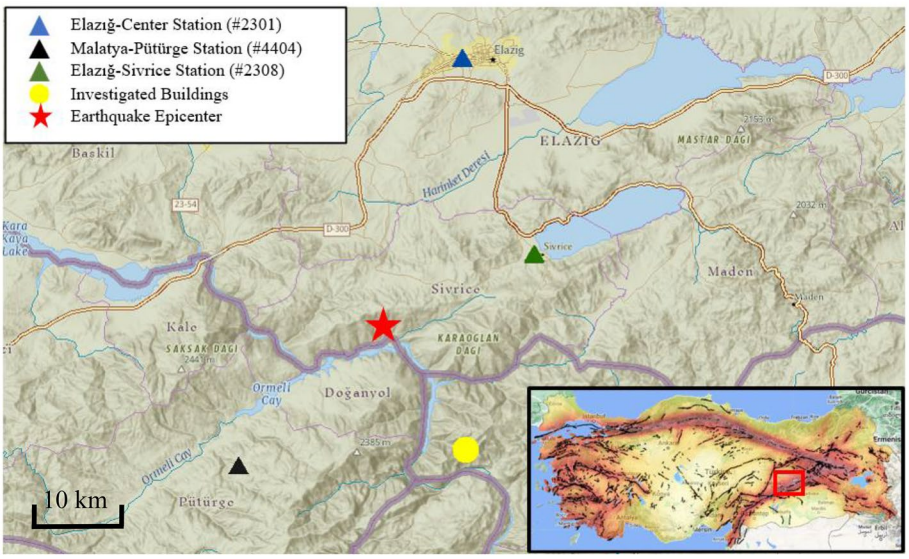

Fig. 1 Coordinates of the Sivrice-Elazığ earthquake epicenter, station for records, and investigated buildings (DEMP(2020))

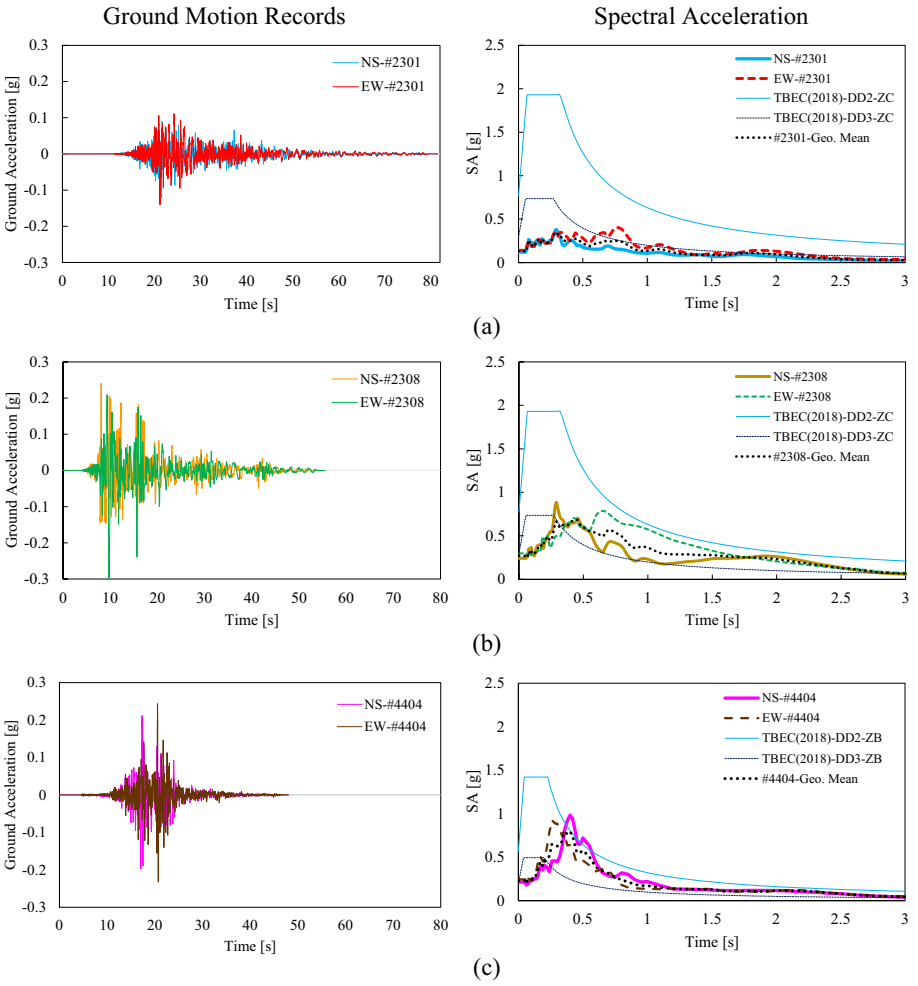

Fig. 2 Time variation of horizontal accelerations and spectral accelerations for **a** Elazığ-Center Station (#2301), **b** Elazığ-Sivrice Station (#2308), and **c** Malatya-Pütürge Station (#4404) during the 2020 Sivrice-Elazığ Earthquake (DEMP (2020)) (DD2: 475-Year Return Period Earthquake, DD3: 72-Year Return Period Earthquake, ZB: stiff soil, ZC: medium-stiff soil)

4 Description of buildings

The two investigated nominally identical RC buildings are located in Karakaya Dam Administration and Operation Campus, Elazığ, Turkey. The buildings were constructed side-by-side in the same period. Therefore, except for the additional structural walls as for retrofitting applied on one of the two buildings, both have identical structural systems/design, material properties, construction practices, and soil conditions. As the retrofitted and non-retrofitted buildings are located in the same place, the soil profile of the two buildings is similar; stiff soil conditions are considered to be ZB according to TBEC (2018).

Table 1 Strong ground motion data of the three stations (DEMP (2020))

Station ID	Location	Latitude [°N]	Longitude [°E]	PGA (g)			PGV (cm/s)			R_{epi} [km]	R_{jb} [km]
				N-S	E-W	U-D	N-S	E-W	U-D		
2301	Elazığ-Center	38.6704	39.1927	0.122	0.143	0.068	10.38	13.33	6.34	36.39	30.43
2308	Elazığ-Sivrice	38.4506	39.3102	0.243	0.298	0.194	27.18	47.50	9.71	23.81	17.86
4404	Malatya-Pütürge	38.1989	38.8738	0.211	0.244	0.157	28.86	25.89	17.24	24.55	18.6

Table 2 Comparison of PGA and PGV values between the recorded data and the seismic design values of Turkish Earthquake Hazard Map (TEHM (2018))

Station ID	Location	V_s30 [m/s]	Local site class TBEC (2018)	Geometric mean		DD-2 (475-year RETURN PERIOD EQ)		DD-3 (72-year return period EQ)	
				PGA [g]	PGV [cm/s]	PGA [g]	PGV [cm/s]	PGA [g]	PGV [cm/s]
2301	Elazığ-Center	407	ZC	0.132	11.763	0.383	23.919	0.148	8.921
2308	Elazığ-Sivrice	450	ZC	0.269	35.244	0.622	44.036	0.230	12.853
4404	Malatya-Pütürge	1380	ZB	0.227	24.335	0.651	45.022	0.237	12.718

ZB, stiff soil; *ZC*, medium-stiff soil

The identical buildings (see Fig. 3a, b) comprise the most common deficiencies of ordinary 3–5 story pre-1990s structures with substandard configuration. In most cases, the concrete strength was significantly below the code-specified values in these buildings due to in-situ mixed concrete with improper aggregate size, excessive water-cement ratio, and lack of curing (Çağatay 2005; Bal et al. 2008). The use of plain round bars, together with insufficient longitudinal and transverse reinforcement detailing, results from poor workmanship and an unaudited construction process. Such conflicts between seismic design code requirements and applications lead to non-conforming configurations. The geometric characteristics of the investigated buildings also reflect the common properties of 3–5-story pre-1990s substandard structures. A summary of Turkish building stock with the statistical outcomes and comparison with properties of the investigated buildings are presented in Table 3. Note that both retrofitted and non-retrofitted buildings have the same properties presented in the third column of Table 3.

The floor plans of the investigated buildings in this study are given in Fig. 4a, b**.** Structural intervention with the addition of the structural walls during the period of 2011–2015 was carried out on the retrofitted residential building. The building that is under the control of another administrative unit was not subject to any structural intervention and remained untouched. The concrete and steel grades used in the additional structural walls of the retrofitted buildings are C25 and S420, respectively. Structural walls were placed in the most symmetrical way as possible, as shown in Fig. 4b.

5 Comparison of earthquake damage

Figure 5 shows the location of severely damaged infill walls together with the counterpart infill walls of the retrofitted building on the structural floor plan. The indoor images in Fig. 6 present the side-by-side damage level of some nonstructural walls in the retrofitted and non-retrofitted buildings after the Sivrice-Elazığ earthquake. The photographic documentation shows the state of infill walls in the non-retrofitted building, which was subject to severe damage or even partial collapse. Due to heavy damage in the infill walls, the non-retrofitted building was not serviceable after the earthquake. In turn, no significant damage

(a) (b)

Fig. 3 Investigated buildings **a** non-retrofitted **b** retrofitted

Table 3 Properties of ordinary substandard buildings and comparison with the investigated buildings

Parameter	Building stock		Investigated buildings	Remarks
	Mean μ	Coefficient of variation C_v		
Story height [m]*	2.87	0.10	2.90	Identical in each story
Long plan dimension [m]*	14.19	0.19	22.70	Relatively large building (see floor plans in Fig. 4.)
Short plan dimension [m]*	9.81	0.21	14.85	
Column width [mm]*	255	0.08	300	See Fig. 4a for positions and orientation
Column depth [mm]*	535	0.25	500, 600, 700	
Number of columns per building area [#/100m^2]*	13.17	0.21	10.68	36 columns per story
Beam width [mm]*	230	0.33	250	
Beam depth [mm]*	531	0.16	500	
Amount of infill-long plan dimension [m/100m^2]*	10.98	0.63	14.88	Hollow clay bricks with mortar and plaster
Amount of infill-short plan dimension [m/100m^2]*	5.13	0.71	22.33	
Longitudinal reinforcement steel ratio*	1.00%	0.19	1.00%	
Reinforcing steel yield strength [MPa]*	222.1	0.09	220	
Concrete compressive strength [MPa]$^{\#}$	10.64	N/A	10	In some extracted cores, 14 MPa

Data from *Ozmen et al. (2015) and $^{\#}$Maziligüney et al. (2008)

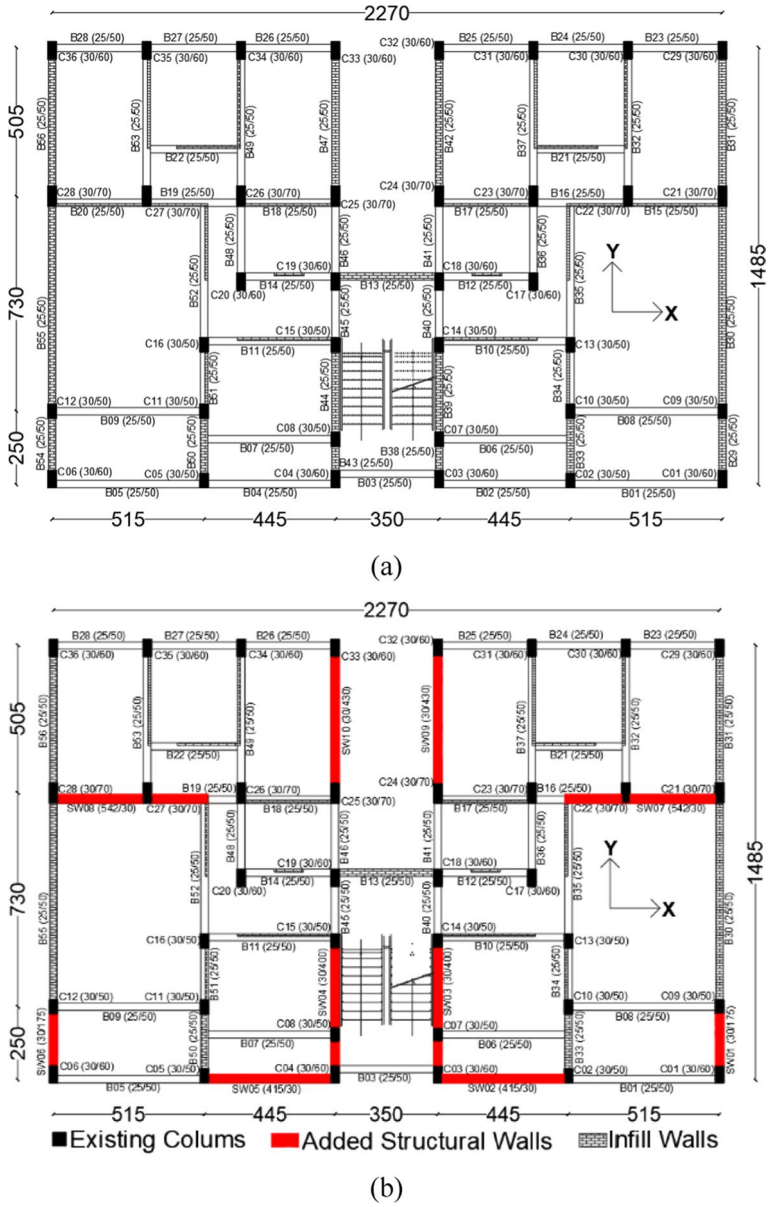

Fig. 4 Floor plan of investigated buildings **a** non-retrofitted **b** retrofitted (units are in [cm])

was detected in the retrofitted building except for the interface cracks between the existing structural components and the additional structural walls, which could be repaired easily after the earthquake without disrupting the serviceability of the building.

The infill wall damage in the non-retrofitted building was mainly concentrated in the x-direction (e.g., along the long plan dimension), as shown in Fig. 6 (see Fig. 5, Wall ID of A and B, and E to H for locations). The infill cracks in the X-pattern were the most

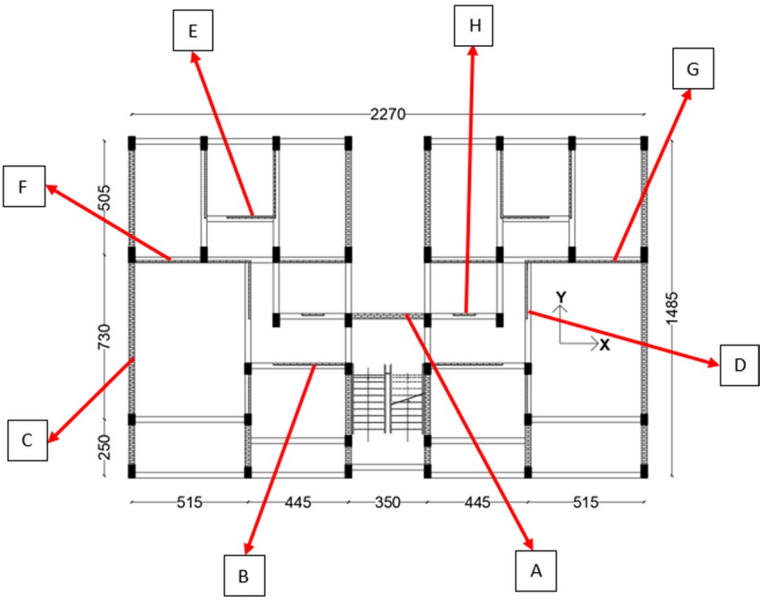

Fig. 5 Position of the damaged infill walls in Fig. 6 on the floor plan

common crack type in the x-direction of the non-retrofitted building. The cracks in the infill walls along the y-direction (e.g., along the short plan dimension) of the non-retrofitted building in Fig. 6 (see Fig. 5, Wall ID of C and D for locations) were formed as interface cracks between the infill masonry and framing members. In the retrofitted building, no/slight cracks were observed for the same walls of A, B, E, and H in the x-direction. The y-direction cracks in retrofitted buildings formed as interface cracks with low intensity. These interface cracks are considered to be indicators of the load transfer from the existing structural system to the additional structural walls.

The on-site investigations carried out after the earthquake clearly demonstrated the effectiveness of structural walls in enhancing the serviceability limit states of retrofitted structures. In particular, the retrofitted building showed only minor cracks, which required cosmetic repairs without interrupting the serviceability of the structure. On the other hand, the non-retrofitted building suffered severe infill damage, rendering the building unserviceable.

6 Numerical models

The numerical models were generated for both retrofitted and non-retrofitted buildings in SeismoStruct (v2022). This programme was used due to the capability of predicting the large displacement behavior of space frames (i.e., models generated with beam-column elements) under static or dynamic loading. The models unveiled the reason behind the different seismic responses observed during the site investigations after the earthquake numerically. The crucial role of infill walls in the structural response, which

Fig. 6 Damage of the retrofitted and non-retrofitted buildings

can cause and trigger various failure mechanisms, is the subject of literature (Hermanns et al. 2013; Seyed Razzaghi and Javidnia 2015). Therefore, the structures were modeled by incorporating the masonry infill walls to reproduce their contribution and influence on seismic behavior. In addition, SeismoStruct offers the user the ability to employ both

Fig. 6 (continued)

geometric nonlinearity and material inelasticity by exploring the structural response under various loading conditions.

6.1 Modeling of structural members

Structural element models were generated by introducing fiber-based beam-column members. Then, at each fiber of the cross-section, a uniaxial stress–strain relationship was assigned for unconfined and confined concrete, as well as for reinforcement steel. Next, the entire sectional stress–strain relationship was obtained through the integration of the individual fibers along the member length. Mander et al.'s (1988) model was employed for the unconfined and confined concrete models, while the reinforcing bars were modeled using the cyclic steel model presented by Menegotto and Pinto (1973). Mechanical properties of the materials and geometric dimensions of the members were examined and determined based on the blueprints of the buildings, with additional data obtained during the field reconnaissance and on-site measurements. The resulting 3D view of the numerical models for both non-retrofitted and retrofitted buildings can be seen in Fig. 7a, b.

6.2 Modeling of infill walls

As confirmed by the field observations, the infill walls consisted of partial hollow clay bricks with mortar and plaster. In SeismoStruct, a four-node infill panel element developed by Crisafulli (1997) was used for the numerical modeling of infill walls (Fig. 8). Specifically, there are a total of six strut members in each infill panel, including axial and shear struts. The infill walls were assumed to be classified as fair-quality infills outlined by FEMA 356 (2000). Thus, the modulus of elasticity, compressive strength, and shear strength of masonry infill walls were taken as 1155, 2.1, and 0.09 MPa, respectively, which is compatible with FEMA 356 (2000).

In the calculation of the elastic in-plane stiffness of masonry infill walls, Eqs. (1) and (2) were utilized. In these equations, E_{me} is the expected modulus of elasticity of the material, I_{col} is the moment of inertia of the column, t_{inf} is the thickness of the infill panel and equivalent strut, θ is the angle whose tangent is the infill height to length aspect ratio (in radian),

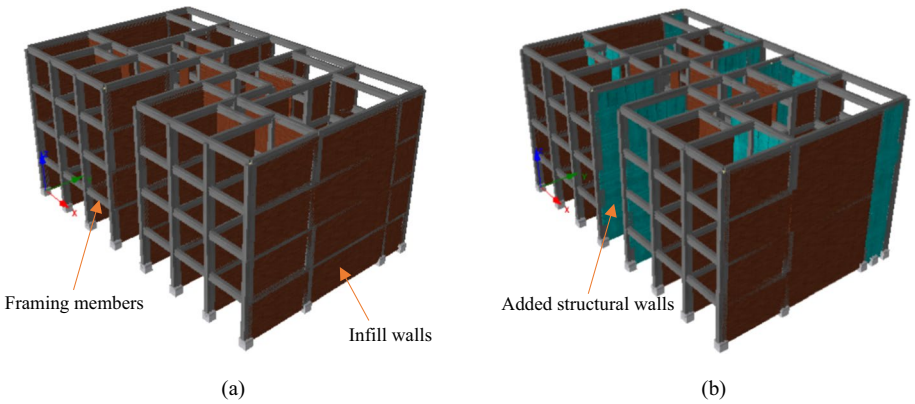

Fig. 7. 3D numerical models **a** non-retrofitted **b** retrofitted building

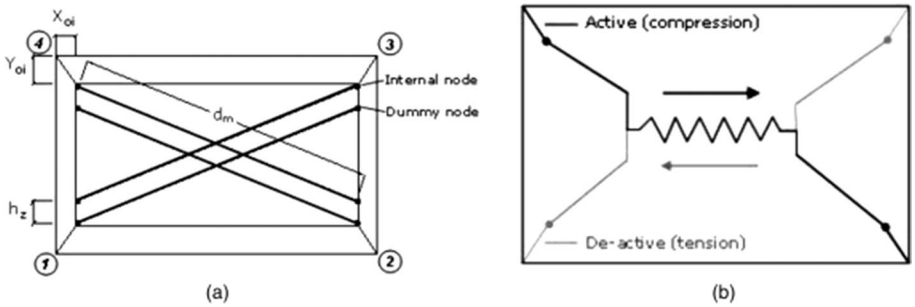

Fig. 8 A four-node masonry infill element **a** compression/tension struts **b** shear struts (SeismoStruct (v2022))

h_{inf} is the height of infill panel, α is the strut width, h_{col} is the column height between centerlines of beams, r_{inf} is the diagonal length of the infill panel, and $\lambda 1$ is defined by FEMA 356 (2000) to compute the equivalent width of the infill strut. The tensile strength of the infills was ignored, and the strain at maximum stress, and the ultimate strain were taken as 0.001 and 0.01, respectively. For the shear spring model, the maximum shear resistance (τ_{max}) was estimated using the formula given in Eq. (3), where the shear bond strength of the infill walls (τ_o) was introduced. The shear bond strength was conservatively taken as 0.3 MPa by default introduced in SeismoStruct.

$$\lambda_1 = \left[\frac{E_{me} t_{inf} sin2\theta}{4E_{fe} I_{col} h_{inf}}\right]^{1/4} \tag{1}$$

$$a = 0.175(\lambda_1 h_{col})^{-0.4} r_{inf} \tag{2}$$

$$\tau_{max} = \tau_0 + 0.3(MPa) \tag{3}$$

The presence of openings around the infill walls can impact the seismic response of the buildings. To that end, the reduction in the strength and stiffness due to the openings was applied to the panel members following the method suggested by Decanini et al. (2014). Herein, the proposed reduction percentage is a function of the opening dimensions and the reinforcing condition of the elements around the openings (Akın 2018). Detailed information on the modeling approach and panel material property in modeling a substandard RC residential building with infills can be found in Duran et al. (2020).

6.3 Details of structural analysis

The eigenvalue, static pushover, and nonlinear response history analyses were conducted to explore the difference between the seismic response of the investigated buildings. The modal properties of both buildings were estimated using the eigenvalue analysis, followed by the pushover analysis. In the pushover analyses, the displacements are increased with small intervals up to the ultimate displacement capacity of the buildings. On the other hand, the actual behavior of the buildings can be better represented by performing a nonlinear response history analysis under the given earthquake ground motion records. In this

study, three earthquake ground motions, which have the highest seismic intensities in terms of PGA among the recorded motions during the earthquake, were used. The earthquake ground motions recorded in Elazığ-Center (Station ID: #2301), Elazığ-Sivrice (Station ID: #2308), and Malatya-Pütürge (Station ID: #4404) were used in the nonlinear response history analysis. The acceleration-time series and response spectra of both horizontal components of the ground motion records are shown in Fig. 2a–c. The North–South (NS) and East–West (EW) acceleration time series of the Elazığ- Sivrice- earthquake were acquired from the Turkey Acceleration Database and Analysis System (TADAS (2020)) for the nonlinear response history analysis. Bi-directional response history analyses were performed with the two horizontal components of each selected ground motion record using the 3D analytical model of the buildings. Indeed, matching the NS and EW components of the ground motions with the building orientations is challenging. Based on the observed infill wall damage presented in Fig. 6, the infill walls that are along the x-direction of the buildings (i.e., long plan dimension) suffered more from the earthquake action. In addition, the non-retrofitted building has the largest period in the x-direction (i.e., long plan dimension) due to its considerably lower stiffness in that direction. Therefore, it is expected to see more damage on the infill walls oriented in this direction. Overall, the stronger component of the selected ground motion records is applied in the x-direction of the buildings (i.e., long plan dimension). Since the PGA of the East–West (EW) component of the acceleration time series of the three ground motions records are higher than the North–South (NS) components, as presented in Fig. 2a–c and Table 1, the buildings were subjected to North–South (NS) acceleration time series in the y-direction (i.e., short plan dimension) and East–West (EW) acceleration time series in the x-direction (i.e., long plan dimension). Constant viscous damping of 5% is considered in the response history analysis.

7 Discussion of analysis results

7.1 Results of eigenvalue and static pushover analysis

Table 4 shows the outcomes of the modal analysis results for the non-retrofitted and retrofitted buildings. The addition of structural walls in the retrofitted building reduced the fundamental period by three to four times in each building's orthogonal component, as a result of increased stiffness. Such a distinct change in the fundamental period values is an expected outcome of the contribution of additional structural walls in the building stiffness. The increase in the stiffness of the retrofitted building resulted in reduced displacement

Table 4 Eigenvalue analysis outcomes of non-retrofitted and retrofitted buildings

Mode number	Retrofit scheme	Period [s]	Mass participation ratio [%]
Mode-1 (x-direction)	Non-retrofitted	0.601	85.76
	Retrofitted	0.136	52.34
Mode-2 (y-direction)	Non-retrofitted	0.415	81.00
	Retrofitted	0.139	70.19
Mode-3 (Torsion)	Non-retrofitted	0.471	81.20
	Retrofitted	0.187	55.19

demands in the retrofitted building. The imposed seismic damage on the infill walls of the non-retrofitted building presented in Fig. 6 can be explained by its relatively flexible nature compared to the retrofitted building. However, the mass participation ratio in each mode is reduced in the retrofitted building (Table 4). Therefore, higher modes of the retrofitted building are relatively more pronounced in the seismic response.

The static pushover curves of the two buildings in both their principal axes are shown in Fig. 9. Although the pushover analyses of the retrofitted building did not converge to the roof displacement values before attaining the effective yield displacement capacity of the buildings, the prominent contribution of additional structural walls of the retrofitted building in the capacity and stiffness curves is obvious. There was a substantial increase in the strength and stiffness of the retrofitted building in its principal axes compared to the non-retrofitted building. The difference between the initial stiffness of the retrofitted and non-retrofitted buildings was in good agreement with the variation of their fundamental periods, as presented in Table 4.

7.2 Results of nonlinear response history analysis

The hysteretic curves of the buildings, which represent base shear force versus roof displacement relationship, were graphically obtained for the selected three ground motion recordings in both x- and y-directions (Fig. 10a–c). The retrofitted building exhibited almost a fully elastic response compared to the non-retrofitted building. A certain level of nonlinearity can be seen in the hysteresis curves of the non-retrofitted building with the formation of wider loops. In addition, the initial stiffness of the retrofitted building was approximately ten times higher in the x-direction and five times higher in the y-direction than that of the non-retrofitted building, indicating a substantial contribution of additional structural walls to the lateral stiffness. The contribution of additional shear walls to the capacity appears to be significant as well.

The absolute maximum inter-story drift ratio (IDR) (Fig. 11a–c) and the peak floor acceleration (Fig. 12a–c) in the corresponding story levels were also obtained in the x- and y-directions of the retrofitted and non-retrofitted buildings. The absolute maximum IDR value was then plotted in Fig. 11a–c. The non-retrofitted building in the x-direction indicated higher IDR values than in the y-direction. The non-retrofitted building deformed

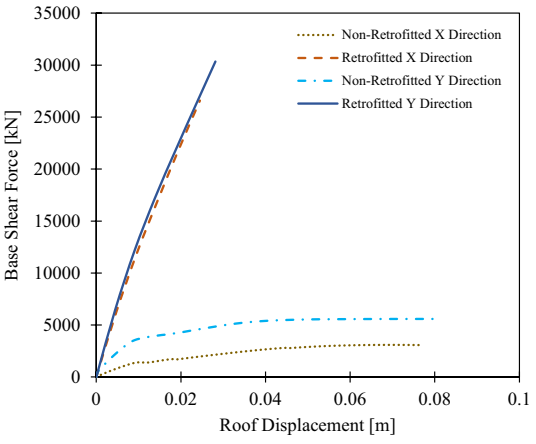

Fig. 9 Static pushover curve of non-retrofitted and retrofitted buildings

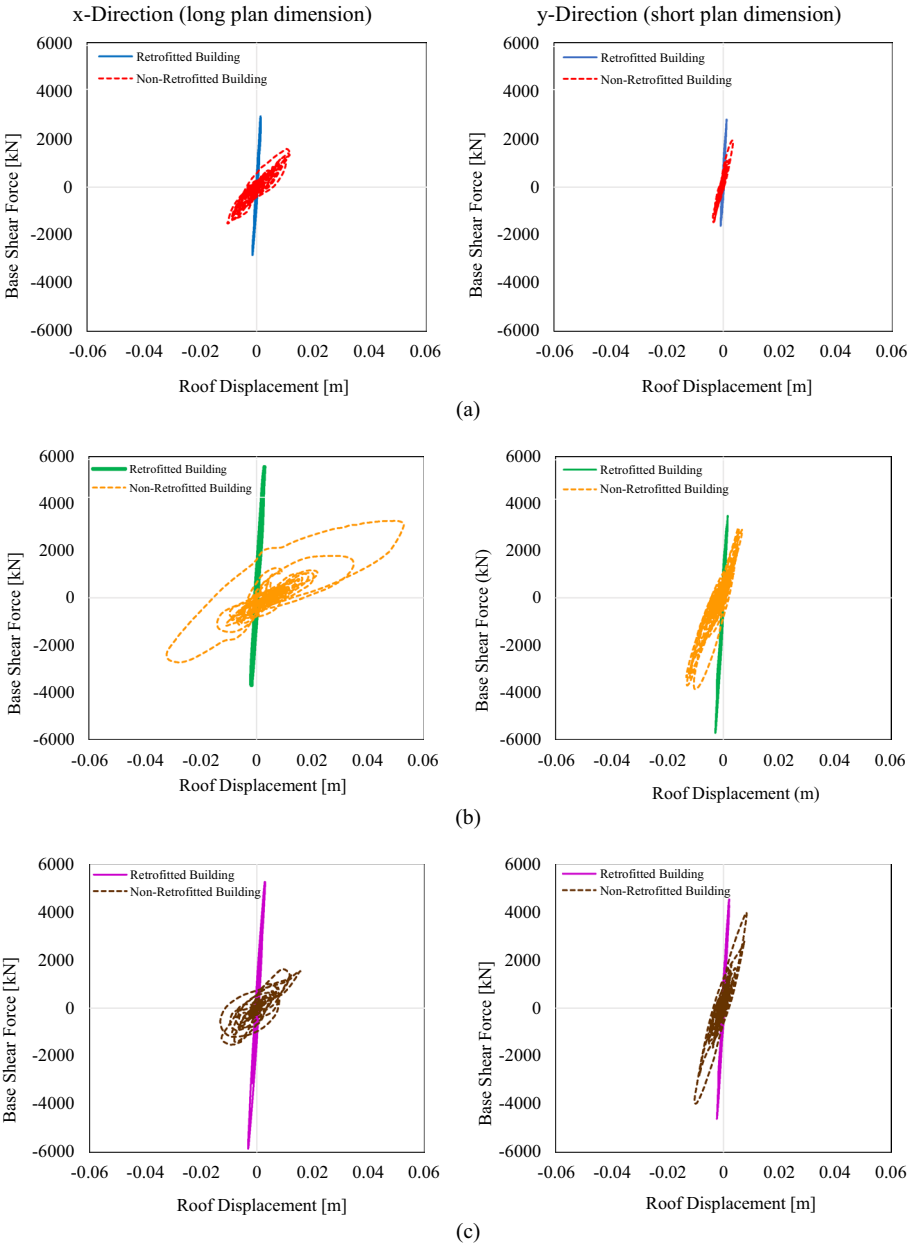

Fig. 10 Hysteresis curves of building models obtained as a result of nonlinear response history analysis in stations **a** Elazığ-Center Station (#2301), **b** Elazığ-Sivrice Station (#2308), and **c** Malatya-Pütürge Station (#4404)

more in the x-direction than the y-direction, concluding that the x-direction is more flexible than the y-direction. This outcome is, indeed, in good agreement with the fundamental periods presented in Table 4, where $T_{x1}=0.601\ s$ and $T_{y1}=0.415\ s$. Furthermore, observing

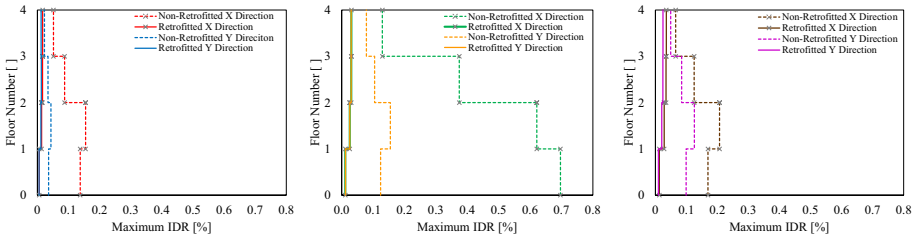

Fig. 11 Variation of maximum IDRs in x- and y-directions of the retrofitted and non-retrofitted buildings in stations **a** Elazığ-Center Station (#2301), **b** Elazığ-Sivrice Station (#2308), and **c** Malatya-Pütürge Station (#4404)

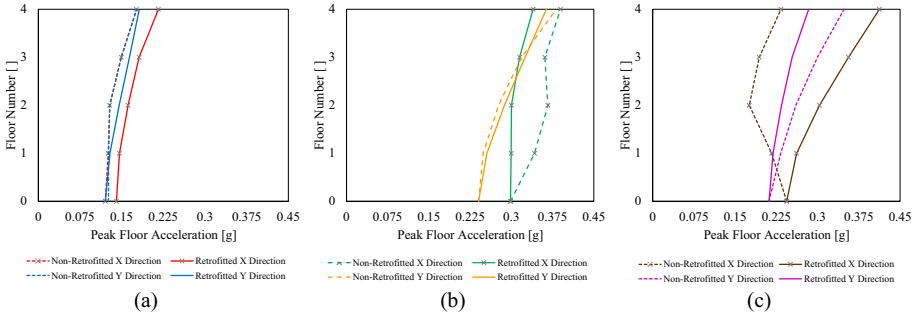

Fig. 12 Variation of peak floor accelerations in x- and y-directions of the retrofitted and non-retrofitted buildings in stations **a** Elazığ-Center Station (#2301), **b** Elazığ-Sivrice Station (#2308), and **c** Malatya-Pütürge Station (#4404)

more damage in the x-direction infill walls of the non-retrofitted building (see Fig. 5-Wall ID of A and B, and E to H for locations, and Fig. 6 for damage level) also complied with the analysis results. Specifically, the increased drift demands in the non-retrofitted building, especially in the x-direction, explain the observed severe damage and partial collapse of the infill walls in the x-direction for the three considered ground motion records. The infill walls of A and B, and E to H, lying in the x-direction shown in Fig. 6, exhibited infill damage dominated by their in-plane behavior. As a result, mainly diagonal cracks were observed in these infill walls. However, the overall behavior of the infill walls of C and D, positioned in the y-direction of the non-retrofitted building, was generally governed by out-of-plane behavior. Therefore, horizontal cracks at the interface of the RC beams and the infill walls were mainly observed in the infill walls of C and D (Fig. 6).

Figure 11a–c visually presents the significant reduction in IDRs of the building retrofitted with additional walls. The reduced story drift demands resulted in a much better seismic behavior of the retrofitted building by preventing imposed damage in the infill walls (Fig. 11a–c). The infill walls of the retrofitted building were protected without experiencing any noticeable damage by the reduced IDR demands. Except for the cosmetic repairs without any high cost and effort, the retrofitted building was serviceable immediately after the earthquake.

The peak floor accelerations were obtained by taking the absolute maximum of the floor accelerations throughout the time span for each earthquake. The difference in the peak floor accelerations of the retrofitted and non-retrofitted buildings was not as distinct as in the case of the variation in maximum IDRs. Depending on the principal direction of the retrofitted building (x- and y-directions) and the ground motion record, the peak floor accelerations can be higher or lower compared to the non-retrofitted building (Fig. 12a–c). For instance, the peak floor accelerations in the x-direction were reduced by retrofitting the building for the Elazığ-Sivrice record (Station ID: #2308), whereas it was just the opposite for the Malatya-Pütürge record (Station ID: #4404).

The demand-capacity ratio was used to evaluate the damage in the structural members. The brittle failure in all structural members (specifically in structural walls due to high shear demand) was checked externally by comparing the peak shear demand (obtained from analyses) to the shear capacity of all members on the basement floor. The shear capacity of the RC columns and beams was computed following TS500 (2000). TBEC (2018) equation was adopted in calculating the shear capacity of the structural walls. The shear demand-to-capacity ratio for the beam, column, and structural wall was found to be lower than 1, indicating no brittle failure of the structural members. That was also congruent with the field observations. The yield chord rotations of columns were calculated based on TBEC (2018), and the flexural damage check was done via chord rotations. The peak chord rotation demands were obtained from the results of time history analysis. It was found that the column chord rotation demands were 44% higher than the yield chord rotation in the average sense. Therefore, the columns were predicted to attain their yield capacity based on the numerical study. However, the observed column damage did not indicate any evidence for yielding. Besides, one should keep in mind that the column chord rotation demands from time history analysis were obtained at the transient peak response of the building. In contrast, the on-site column damages were observed after the earthquake representing the residual deformations of the columns. Therefore, it is very likely to have differences between the numerical simulations and on-site observations of the building, which have slight/no structural damage.

Some local seismic response parameters were also investigated. Since the seismic damage was mostly localized in the infill walls, the axial and shear deformations of the infill

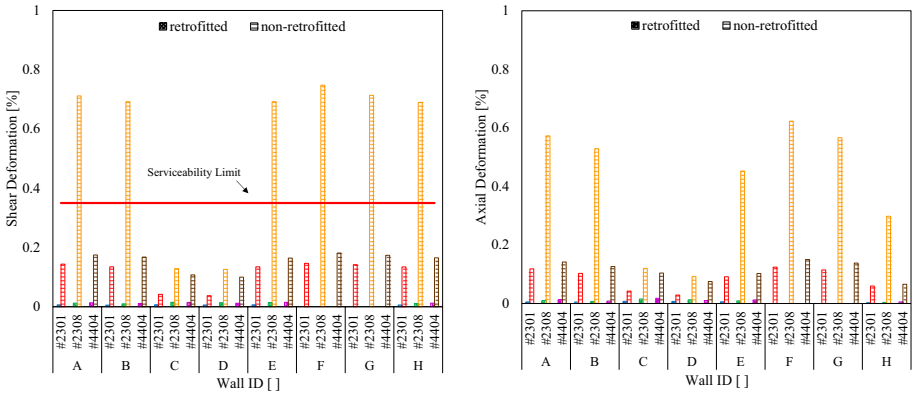

Fig. 13 Investigated infill walls **a** shear deformation **b** axial deformation

walls of A to H shown in Fig. 5 were obtained for the three selected earthquake ground motion records in Fig. 13a and b. Infill shear deformation, which is the relative displacement between the top and bottom of the infill wall divided by its height, namely IDR, was obtained from the two shear struts having the greater shear deformation (Fig. 13a). Axial deformation of the infill walls was obtained from the compression/tension strut elements having the absolute maximum axial elongation or shortening (Fig. 13b). Since the axial and shear deformations of an infill wall are geometrically related, the discussion of the local deformations is focused on the shear deformations of the infill walls. As also indicated in the previous discussion, the Elazığ-Sivrice earthquake record (Station ID: #2308) imposed higher local deformation demands on the infill walls in terms of both axial and shear deformations. The x-direction of the non-retrofitted building is more flexible. Therefore, the corresponding infill walls of A and B, and E to H that lie along the x-direction of the building have higher local seismic demands compared to the infill walls of C and D located in the y-direction of the building. The photographically documented damage levels (i.e., large X-pattern cracks or partial collapse in the x-direction) in these walls are in line with the numerical outcome (Fig. 6 and Fig. 13a). When the local deformation demands imposed on the investigated infill walls of retrofitted and non-retrofitted buildings are compared (Fig. 13a), the local deformations in the infill walls of the non-retrofitted building were a lot more than in the retrofitted ones. This clearly verifies the difference between the observed damage levels in two buildings after the earthquake.

To quantify the numerically obtained local deformations, a deformation limit value was sought through literature and existing codes. In the seismic design codes for new buildings such as TBEC (2018), ASCE 7–16 (2016), and EN 1998–8-1 (2004), IDR of the whole structural system is limited to avoid seismic damage in the building's components for the design level earthquake. Specifically, EN 1998–8-1 (2004) limits the IDR for damage prevention to 0.5, 0.75, and 1.0% for buildings with nonstructural elements of brittle materials, buildings having nonstructural elements, and buildings having nonstructural elements fixed in a way so as not to interfere with structural deformations, or without nonstructural elements, respectively. Qualitative descriptions are defined for the damage states of structural components in EN 1998–8-3 (2005). IDR for the limit state of significant damage for masonry structures is defined as 0.40% for secondary masonry walls and 0.60% for primary seismic walls (EN 1998–8-3 (2005)). In ASCE SEI 41–17 (2017), depending on several parameters such as the ratio of expected frame strength to expected infill strength, aspect ratio of the infill wall, classification of infilled RC frame (frame ductility and relative stiffness of infill wall), deflection relations are specified for the immediate occupancy, life safety, and collapse prevention acceptance criteria. Even though too many parameters are required to apply the ASCE SEI 41–17 (2017) specification, the drift at peak strength for infilled frame bay is also given as 0.35% for flexible nonductile panels. Furtado et al. (2019), referring to FEMA 306 (1998) and FEMA 307 (1998), summarize the damage levels based on IDR, which are 0.25% for no cracking, 0.50% for diagonal cracking, and 1.50% for severe damage. Sucuoğlu (2013) emphasized that 0.4% IDR conforms with the observed severe damage in the infill walls. Griffith (2008) reports that most masonry infills reach their ultimate strength at 0.2%-0.4% IDR. As shown in Fig. 13a, in-plane shear deformations of the investigated infill walls of A and B, and E to H lying in the x-direction of the non-retrofitted building under Elazığ-Sivrice earthquake record (Station ID: #2308) are much higher than the limits in the literature. Specifically, the computed shear deformation is almost double that of the ASCE SEI 41–17 (2017) limit. This can explain the severe damage and partial collapse of the infill walls of the non-retrofitted building. On the other hand, the local deformation demands for the retrofitted building are much less than the

deformation limit value due to the increased stiffness of the building with the additional structural walls. Having no/slight damage in the infill walls of the retrofitted building is quantified by the numerical analysis.

The sensitivity of serviceability to the different intensities of the most critical record [#2308] was investigated by a parametric study. The analyses were run with the ground motion pairs scaled with 0.2, 0.4, 0.6, 0.8, and 1.0 for the non-retrofitted building. Then, the shear deformation of the infill walls was monitored. The critical intensity of the record, where at least one wall reaches a serviceability limit of 0.35%, was then evaluated. As seen in Fig. 14, the serviceability limit of the walls in the non-retrofitted building was reached/exceeded when 60% of the most critical record (i.e., #2308) was applied. However, the walls of the retrofitted building did not even reach the serviceability limit state at a 100% scale (see Fig. 13).

8 Conclusion

The Sivrice-Elazığ earthquake, which occurred on January 24th, 2020, affected two side-by-side nominally identical RC residential buildings that have the same material properties, soil condition, and structural configuration and geometry. However, only one of the two buildings had been retrofitted by adding structural walls before the earthquake. To investigate the differences in the seismic damage imposed on both of the buildings, a field survey was conducted following the earthquake. The retrofitted building had significantly lower deformation demand on its infill walls compared to the non-retrofitted building. No/slight damage in the infill walls was apparent in the retrofitted building, while severe damage with partial collapse of infill walls was photographically documented in the non-retrofitted building. The observed difference in the seismic response of the retrofitted and non-retrofitted buildings was well quantified and explored by computer simulations (i.e., eigenvalue, static pushover analyses, and nonlinear response history analyses with the highest seismic intensity parameters among the recorded ground motions). Based on on-site damage observations and the presented numerical study, the following conclusions can be drawn:

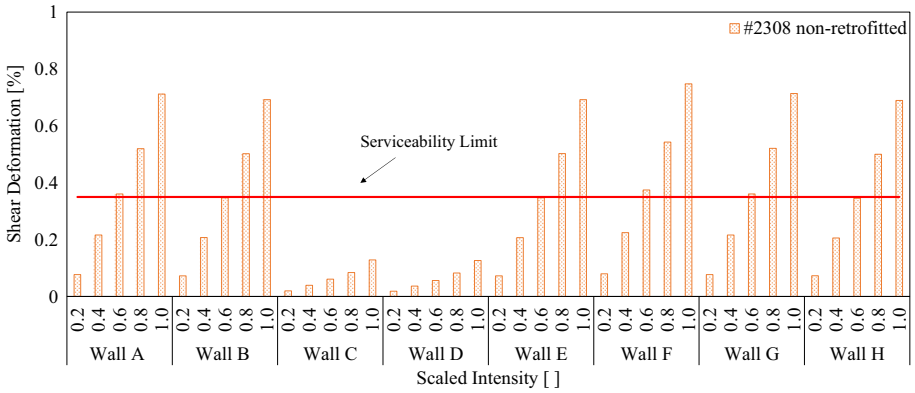

Fig. 14 Shear deformation of infill walls under the different scales of Elazığ-Sivrice record (i.e., Station #2308)

- Although the structural systems of both buildings did not suffer any seismic damage, the infill walls of the non-retrofitted building were subjected to severe damage in the form of X- pattern cracks, and even partial collapse took place. Therefore, the non-retrofitted building was not serviceable, and a considerable amount of repair work and financial resources were necessary to restore it to a functional state after such a moderate-intensity earthquake. However, the imposed local deformations on non-structural components were reduced significantly by the additional structural walls in the retrofitted building. Hence, the retrofitted building was immediately serviceable after the earthquake with only cosmetic repairs needed for the interface cracks.
- The additional structural walls increased the building stiffness, which is also justified by the reduced fundamental period of the retrofitted building obtained from the eigenvalue analysis. The increase in capacity with the provided retrofitting action was significant as well.
- There was a distinct difference in the IDRs calculated from nonlinear response history analyses for the two buildings. The relatively higher IDRs of the non-retrofitted building were the main reason for the severe damage observed in the infill walls.
- The variation in the peak floor accelerations of the two buildings was not as apparent as in the case of IDRs. With the additional structural walls for retrofitting, the peak floor accelerations can be higher or lower depending on the direction of the building and the ground motion record.
- The numerically obtained local deformations of the infill walls, especially under the Elazığ-Sivrice station record (Station ID: #2308), in the non-retrofitted building were much higher than the retrofitted ones. The exposed difference in the responses, which was photographically documented, is quantified by the numerical approach.
- The simulated deformation in the non-retrofitted building was beyond the serviceability criterion defined in the recognized literature for damage-proof infill walls. Limiting the imposed deformations by increasing the building stiffness decreases the infill deformation demand. Thus, the infills can be serviceable without any downtime since they do not go beyond their serviceable limits.

The numerical study simulated the response of non-conforming buildings with common deficiencies and non-seismic details. It is recognized that the adopted modeling strategy may not account for all deformations in structural members. Additionally, the post-earthquake investigation was based on visual inspections. While this method provided valuable information on the actual performance of the buildings, it is important to quantify the uncertainty associated with the visual inspection data.

Acknowledgements This study has been accomplished with the support of the University of Pardubice.

Author contribution AŞ: Methodology, Software, ÖY: Conceptualization, Writing—Original draft preparation, BD: Software, Validation, OT: Data collection, Visualization, SY: Data collection, ÖA: Reviewing and Editing, Supervision.

Funding Open access publishing supported by the National Technical Library in Prague. The authors have not disclosed any funding.

Data availability statement Some or all data, models, or codes that support the findings of this study are available from the corresponding author or other authors upon reasonable request.

Declarations

Conflict of interest The authors declare that they have no known competing financial interests or personal relationships that could have appeared to influence the work reported in this study.

References

Akbari R, Aboutalebi MH, Maheri M (2015) Seismic fragility assessment of steel X-braced and chevron-braced RC frames. Asian J Civil Eng 16:13–27

Akın E (2018) Effects of various parameters on nonlinear dynamic response of infilled RC buildings with open ground story. Thessaloniki, Greece, p 12

Altin S, Anil Ö, Kara ME (2008) Strengthening of RC nonductile frames with RC infills: an experimental study. Cement Concr Compos 30:612–621. https://doi.org/10.1016/j.cemconcomp.2007.07.003

Anadolu Agency (2020) Death toll from earthquake in Turkey rises to 41. Anadolu Agency. Retrieved 27 January 2020

ASCE/7–16 (2016) Minimum design loads and associated criteria for buildings and other structures. American Society of Civil Engineers, Reston, VA

ASCE SEI41 (2017) Seismic evaluation and retrofit of existing buildings. American Society of Civil Engineers, Reston, VA

Avşar Ö, Tunaboyu O (2013) Influence of structural wall on the seismic performance of RC buildings during the May 19, 2011 Simav, Turkey earthquake. ASCE J Perform Constr Facil 28:9. https://doi.org/10.1061/(ASCE)CF.1943-5509.0000473

Bal İE, Crowley H, Pinho R, Gülay FG (2008) Detailed assessment of structural characteristics of Turkish RC building stock for loss assessment models. Soil Dyn Earthq Eng 28:914–932. https://doi.org/10.1016/j.soildyn.2007.10.005

Çağatay İH (2005) Experimental evaluation of buildings damaged in recent earthquakes in Turkey. Eng Fail Anal 12:440–452. https://doi.org/10.1016/j.engfailanal.2004.02.007

Cao X-Y, Shen D, Feng D-C et al (2022) Seismic retrofitting of existing frame buildings through externally attached sub-structures: State of the art review and future perspectives. J Build Eng 57:104904. https://doi.org/10.1016/j.jobe.2022.104904

CEN (2004) Design of structures for earthquake resistance - Part 1: General rules, seismic actions and rules for buildings. EN1998–1. Comité Européen de Normalisation (CEN). Brussels, Belgium

CEN (2005) Design of structures for earthquake resistance - Part 3: Assessment and retrofitting of buildings. EN1998–3. Comité Européen de Normalisation (CEN). Brussels, Belgium

Cerè G, Rezgui Y, Zhao W, Petri I (2022) Shear walls optimization in a reinforced concrete framed building for seismic risk reduction. J Build Eng 54:104620. https://doi.org/10.1016/j.jobe.2022.104620

Crisafulli F (1997) Seismic behaviour of reinforced concrete structures with masonry infills. Ph.D. Thesis, University of Canterbury

De Risi MT, Del Vecchio C, Ricci P et al (2020) Light FRP strengthening of poorly detailed reinforced concrete exterior beam–column joints. J Compos Constr 24:04020014. https://doi.org/10.1061/(ASCE)CC.1943-5614.0001022

Decanini LD, Liberatore L, Mollaioli F (2014) Strength and stiffness reduction factors for infilled frames with openings. Earthq Eng Eng Vib 13:437–454. https://doi.org/10.1007/s11803-014-0254-9

Del Vecchio C, Di Ludovico M, Balsamo A et al (2014) Experimental investigation of exterior RC beam-column joints retrofitted with FRP systems. J Compos Constr 18:04014002. https://doi.org/10.1061/(ASCE)CC.1943-5614.0000459

Del Zoppo M, Di Ludovico M, Balsamo A et al (2017) FRP for seismic strengthening of shear controlled RC columns: Experience from earthquakes and experimental analysis. Compos B Eng 129:47–57. https://doi.org/10.1016/j.compositesb.2017.07.028

DEMP (2020) 24 January 2020 Sivrice (Elazığ) Earthquake Report (in Turkish). Disaster and Emergency Management Presidency (DEMP), Turkey

Duran B, Tunaboyu O, Atli KC, Avşar Ö (2019) Seismic performance upgrading of substandard RC frames using shape memory alloy bars. Smart Mater Struct 28:085007. https://doi.org/10.1088/1361-665X/ab28f6

Duran B, Tunaboyu O, Avşar Ö (2020) Structural failure evaluation of a substandard RC building due to basement story short-column damage. J Perform Constr Facil 34:15. https://doi.org/10.1061/(ASCE)CF.1943-5509.0001455

Durucan C, Dicleli M (2010) Analytical study on seismic retrofitting of reinforced concrete buildings using steel braces with shear link. Eng Struct 32:2995–3010. https://doi.org/10.1016/j.engstruct.2010.05.019

FEMA 306 (1998) Evaluation of earthquake damaged concrete and masonry wall buildings: basic procedures manual (FEMA 306). Federal Emergency Management Agency, USA

FEMA 307 (1998) Evaluation of earthquake damaged concrete and masonry wall buildings: technical resources (FEMA 307). Federal Emergency Management Agency, USA

FEMA 356 (2000) Prestandard and commentary for the seismic rehabilitation of buildings (FEMA 356). Federal Emergency Management Agency, USA

Furtado A, Vila-Pouca N, Varum H, Arêde A (2019) Study of the seismic response on the infill masonry walls of a 15-storey reinforced concrete structure in Nepal. Buildings 9:39. https://doi.org/10.3390/buildings9020039

Garcia R, Hajirasouliha I, Pilakoutas K (2010) Seismic behaviour of deficient RC frames strengthened with CFRP composites. Eng Struct 32:3075–3085. https://doi.org/10.1016/j.engstruct.2010.05.026

Griffith M (2008) Seismic retrofit of RC frame buildings with masonry infill walls: Literature review and preliminary case study. EUR 23289 EN. OPOCE; 2008. JRC44166. Luxembourg (Luxembourg)

Hermanns L, Fraile A, Alarcón E, Álvarez R (2013) Performance of buildings with masonry infill walls during the 2011 Lorca earthquake. Bull Earthq Eng 12:1977–1997. https://doi.org/10.1007/s10518-013-9499-3

Joseph R, Mwafy A, Alam MS (2022) Seismic performance upgrade of substandard RC buildings with different structural systems using advanced retrofit techniques. J Build Eng 59:105155. https://doi.org/10.1016/j.jobe.2022.105155

Kaltakci M, Arslan M, Yilmaz U, Arslan H (2008) A new approach on the strengthening of primary school buildings in Turkey: An application of external shear wall. Build Environ 43:983–990. https://doi.org/10.1016/j.buildenv.2007.02.009

Kara M, Altin S (2006) Behavior of reinforced concrete frames with reinforced concrete partial infills. ACI Struct J 103:701–709

Lee DH, Han S-J, Kim KS, LaFave JM (2017) Shear strength of reinforced concrete beams strengthened in shear using externally-bonded FRP composites. Compos Struct 173:177–187. https://doi.org/10.1016/j.compstruct.2017.04.025

Maheri M, Kousari R, Razazan M (2003) Pushover tests on steel X-braced and knee-braced RC frames. Eng Struct 25:1697–1705. https://doi.org/10.1016/S0141-0296(03)00150-0

Mander JB, Priestley MJN, Park R (1988) Theoretical stress-strain model for confined concrete. J Struct Eng 114:1804–1826. https://doi.org/10.1061/(ASCE)0733-9445(1988)114:8(1804)

Maziligüney L, Yaman I, Azılı F (2008) In-situ concrete compressive strength of residential, public and military structures. Famagusta, North Cyprus

Mazzolani F, Della Corte G, D'Aniello M (2009) Experimental analysis of steel dissipative bracing systems for seismic upgrading. J Civ Eng Manag 15:7–19. https://doi.org/10.3846/1392-3730.2009.15.7-19

Menegotto M, Pinto PE (1973) Method of analysis for cyclically loaded R.C. plane frames including changes in geometry and non-elastic behaviour of elements under combined normal force and bending. https://doi.org/10.5169/SEALS-13741

MoEU (2020) Ministry Environment and Urbanisation, Republic of Turkey. https://csb.gov.tr/

Naseer A, Khan A, Hussain Z, Ali Q (2010) Observed seismic behavior of buildings in Northern Pakistan during the 2005 Kashmir earthquake. Earthquake Spectra 26. https://doi.org/10.1193/1.3383119

Ozmen H, Inel M, Senel S, Kayhan A (2015) Load carrying system characteristics of existing Turkish RC building stock. Int J Civil Eng 13:76

Ozturk M (2013) Field reconnaissance of the October 23, 2011, Van, Turkey, earthquake: Lessons from structural damages. J Perform Constr Facil 29:04014125. https://doi.org/10.1061/(ASCE)CF.1943-5509.0000532

Ricci P, De Luca F, Verderame GM (2011) 6th April 2009 L'Aquila earthquake, Italy: reinforced concrete building performance. Bull Earthquake Eng 9:285–305. https://doi.org/10.1007/s10518-010-9204-8
Rossetto T, Peiris N (2009) Observations of damage due to the Kashmir earthquake of October 8, 2005 and study of current seismic provisions for buildings in Pakistan. Bull Earthquake Eng 7:681–699. https://doi.org/10.1007/s10518-009-9118-5
SeismoStruct (v2022) A Computer Program for Static and Dynamic Nonlinear Analysis of Framed Structures.
Seyed Razzaghi M, Javidnia M (2015) Evaluation of the effect of infill walls on seismic performance of RC dual frames. Int J Adv Struct Eng (IJASE) 7:49–54. https://doi.org/10.1007/s40091-015-0081-x
Shahzada K, Khan A, Elnashai A et al (2010) Dynamic response of confined brick masonry buildings. In: Dynamic Response of Confined Brick Masonry Buildings
Sonuvar MO, Ozcebe G, Ersoy U (2004) Rehabilitation of reinforced concrete frames with reinforced concrete infills. ACI Struct J 101:494–500
Strepelias E, Palios X, Bousias S, Fardis M (2014) Experimental investigation of concrete frames infilled with RC for seismic rehabilitation. J Struct Eng 140:04013033. https://doi.org/10.1061/(ASCE)ST.1943-541X.0000817
Sucuoglu H (2013) Implications of masonry infill and partition damage in performance perception in residential buildings after a moderate earthquake. Earthq Spectra 29:661–667. https://doi.org/10.1193/1.4000147
TADAS (2020) Turkish Accelerometric Database and Analysis System (TADAS), Turkey. Retrieved 18 June 2020. https://tadas.afad.gov.tr/event-detail/8071
TBEC (2018) Turkish Building Earthquake Code, Specification for structures to be built in disaster areas: Ministry of Public Works and Settlement Government of Republic of Turkey, Ankara, Turkey
TEHM (2018) Turkish Earthquake Hazard Map. https://tdth.afad.gov.tr
Thermou GE, Elnashai AS (2006) Seismic retrofit schemes for RC structures and local–global consequences. Earthquake Eng Struct Dynam 8:1–15. https://doi.org/10.1002/pse.208
TS500 (2000) Requirements for design and construction. Turkish Standard Institution
Yılmaz N, Avşar Ö (2013) Structural damages of the May 19, 2011, Kütahya-Simav earthquake in Turkey. Nat Hazards 69:981–1001. https://doi.org/10.1007/s11069-013-0747-2
Yurdakul Ö, Duran B, Tunaboyu O, Avşar Ö (2021) Field reconnaissance on seismic performance of RC buildings after the January 24, 2020 Elazığ-Sivrice earthquake. Nat Hazards 105:1–29. https://doi.org/10.1007/s11069-020-04340-x
Yurdakul Ö, Tunaboyu O, Routil L, Avşar Ö (2019) Stochastic-based nonlinear numerical modeling of shear critical RC beam repaired with bonded CFRP sheets. J Compos Constr 23:04019042. https://doi.org/10.1061/(ASCE)CC.1943-5614.0000966
Yurdakul Ö, Tunaboyu O, Routil L, Avşar Ö (2020) Parameter sensitivity of CFRP retrofitted substandard joints by stochastic computational mechanics. Composite Structures 238:112003. https://doi.org/10.1016/j.compstruct.2020.112003

Authors and Affiliations

Ahmet Şimşek[1] · Özgür Yurdakul[2] · Burak Duran[3] · Onur Tunaboyu[1] · Suat Yıldırım[4] · Özgür Avşar[1]

✉ Özgür Yurdakul
ozgur.yurdakul@upce.cz

Ahmet Şimşek
ahmet_simsek@ogr.eskisehir.edu.tr

Burak Duran
burak.duran@unh.edu

Onur Tunaboyu
onurtunaboyu@eskisehir.edu.tr

Suat Yıldırım
syildirim@promerengineering.com.tr

Özgür Avşar
ozguravsar@eskisehir.edu.tr

[1] Eskişehir Technical University, Eskişehir, Turkey

[2] University of Pardubice, Pardubice, Czech Republic

[3] University of New Hampshire, Durham, NH, USA

[4] Promer Engineering, Ankara, Turkey